1521-009X/49/7/572–580$35.00
DRUG METABOLISM AND DISPOSITION

https://doi.org/10.1124/dmd.121.000381
Drug Metab Dispos 49:572–580, July 2021

Nonclinical Pharmacokinetics and Absorption, Distribution, Metabolism, and Excretion of Givosiran, the First Approved *N*-Acetylgalactosamine–Conjugated RNA Interference Therapeutic

Jing Li, Ju Liu, Xuemei Zhang, Valerie Clausen, Chris Tran, Michael Arciprete, Qianfan Wang, Carrie Rocca, Li-Hua Guan, Guodong Zhang, Diana Najarian, Yuanxin Xu, Peter Smith, Jing-Tao Wu, and Saeho Chong

Alnylam Pharmaceuticals Inc., Cambridge, Massachusetts

Received January 19, 2021; accepted April 19, 2021

ABSTRACT

Givosiran is an *N*-acetylgalactosamine–conjugated RNA interference therapeutic that targets 5′-aminolevulinate synthase 1 mRNA in the liver and is currently marketed for the treatment of acute hepatic porphyria. Herein, nonclinical pharmacokinetics and absorption, distribution, metabolism, and excretion properties of givosiran were characterized. Givosiran was completely absorbed after subcutaneous administration with relatively short plasma elimination half-life ($t_{1/2}$; less than 4 hours). Plasma exposure increased approximately dose proportionally with no accumulation after repeat doses. Plasma protein binding was concentration dependent across all species tested and was around 90% at clinically relevant concentration in human. Givosiran predominantly distributed to the liver by asialoglycoprotein receptor–mediated uptake, and the $t_{1/2}$ in the liver was significantly longer (~1 week). Givosiran was metabolized by nucleases, not cytochrome P450 (P450) isozymes, across species with no human unique metabolites. Givosiran metabolized to form one primary active metabolite with the loss of one nucleotide from the 3′ end of antisense strand, AS(N-1)3′ givosiran, which was equipotent to givosiran. Renal and fecal excretion were minor routes of elimination of givosiran as approximately 10% and 16% of the dose was recovered intact in excreta of rats and monkeys, respectively. Givosiran is not a substrate, inhibitor, or inducer of P450 isozymes, and it is not a substrate or inhibitor of uptake and most efflux transporters. Thus, givosiran has a low potential of mediating drug-drug interactions involving P450 isozymes and drug transporters.

SIGNIFICANCE STATEMENT

Nonclinical pharmacokinetics and absorption, distribution, metabolism, and excretion (ADME) properties of givosiran were characterized. Givosiran shows similar pharmacokinetics and ADME properties across rats and monkeys in vivo and across human and animal matrices in vitro. Subcutaneous administration results in adequate exposure of givosiran to the target organ (liver). These studies support the interpretation of toxicology studies, help characterize the disposition of givosiran in humans, and support the clinical use of givosiran for the treatment of acute hepatic porphyria.

Introduction

RNA interference (RNAi) is a natural cellular process of gene silencing that represents one of the most promising and rapidly advancing frontiers in biology and drug development today (Wittrup and Lieberman, 2015; Setten et al., 2019; Hu et al., 2020). Small interfering RNA (siRNA), which mediates RNAi, is a class of short, noncoding, double-stranded RNA that can suppress gene expression by targeting and degrading mRNA through an RNA-induced silencing complex (Liu et al., 2004; Nakanishi, 2016). RNAi therapeutics offer many advantages, such as being able to target diseases that are not always treatable with small molecules or proteins and being able to specifically target a wide range of genes. Although they showed promise in their infancy, RNAi therapeutics faced many challenges. siRNA is difficult to deliver to its target and easily degraded by RNases if left unmodified. However, advances in RNAi technology have led to deliverable therapeutics that remain stable in the body for several weeks to months (Nair et al., 2017; Foster et al., 2018). To date, four RNAi therapeutics have been approved for human use: patisiran (ONPATTRO) in 2018, givosiran (GIVLAARI) in 2019, and lumasiran (OXLUMO) and inclisiran (Leqvio) in 2020.

Givosiran was approved in the United States for the treatment of acute hepatic porphyria (AHP) in adults and in the European Union for

This work was supported by Alnylam Pharmaceuticals Inc. The authors are, or were during the time this work was conducted, employees and stockholders of Alnylam Pharmaceuticals.

https://dx.doi.org/10.1124/dmd.120.000381.

ABBREVIATIONS: ADME, absorption, distribution, metabolism and excretion; AHP, acute hepatic porphyria; *ALAS1*, 5′-aminolevulinate synthase 1; ASGPR, asialglycoprotein receptor; AS(N-1)3′, double-stranded metabolite of givosiran with loss of one nucleotide from antisense strand 3′ end; AS(N-1)5′, metabolite of givosiran with loss of one nucleotide from the 5′ end of the antisense strand; AS(N-3)5′, metabolite of givosiran with loss of three nucleotides from the 5′ end of antisense strand; AUC, area under the curve; AUC_{last}, area under the plasma concentration-time curve from the time of dosing to the last measurable concentration; CL, total clearance; DDI, drug-drug interaction; EMSA, electrophoretic mobility shift assay; GalNAc, *N*-acetylgalactosamine; LC-HRMS, liquid chromatography coupled with high resolution mass spectrometry; P450, cytochrome P450; PK, pharmacokinetics; PPB, plasma protein binding; RNAi, RNA interference; siRNA, small interfering RNA; $t_{1/2}$, elimination half-life; V_{ss}, volume of distribution at steady state.

the treatment of AHP in adults and adolescents aged 12 years or older. AHP is a rare disease with a prevalence of 5 to 10 cases per 100,000 people in the United States and affects primarily women (age range 15 to 45 years). AHP occurs due to an autosomal dominant mutation that leads to deficiencies in the heme biosynthesis enzymes aminolevulinic acid dehydratase and porphobilinogen deaminase (Puy et al., 2010; Balwani and Desnick, 2012). The rate-limiting step in heme synthesis is catalyzed by the enzyme 5′-aminolevulinate synthase 1 (ALAS1), which is controlled by feedback repression via the end-product heme. In patients with AHP, induction of *ALAS1* results in increased production and accumulation of toxic heme intermediates delta-aminolevulinic acid and porphobilinogen. Clinically, accumulation of these toxic heme intermediates results in acute porphyria attacks characterized by severe abdominal pain, muscle weakness, seizures, psychiatric dysfunction, irreversible neurologic damage, and increased risk of hepatic malignancy (Bissell and Wang, 2015). Givosiran targets and degrades hepatic *ALAS1* mRNA, reducing the production of ALAS1 protein, which in turn prevents the accumulation of toxic delta-aminolevulinic acid and PBG (Chan et al., 2015; Sardh et al., 2019; Balwani et al., 2020).

Unlike patisiran, where targeted delivery to the liver is achieved by encapsulating the siRNA in lipid nanoparticles and administration is by intravenous infusion (Akinc et al., 2019), givosiran is specifically designed for delivery to the liver through conjugation of a triantennary *N*-acetylgalactosamine (GalNAc) ligand to the sense strand of the siRNA and is administered subcutaneously. The GalNAc ligand directs hepatocyte-specific uptake of siRNA via the asialoglycoprotein receptor (ASGPR), which is highly expressed on the surface of hepatocytes (Nair et al., 2014). Givosiran is the first GalNAc-conjugated RNAi therapeutic that has been approved by the US Food and Drug Administration and the European Commission, with the recommended dose of 2.5 mg/kg administered via subcutaneous injection once monthly, and currently many more GalNAc-conjugated RNAi therapeutics are in late-stage clinical development (Setten et al., 2019; Humphreys et al., 2020).

The clinical pharmacokinetics (PK) and pharmacodynamics of givosiran from the phase 1 study in patients with acute intermittent porphyria, the most common AHP type, have been reported (Agarwal et al., 2020). The present paper reports the PK and the absorption, distribution, metabolism, and excretion (ADME) properties of givosiran across multiple matrices in nonclinical species, with a primary focus on rats and monkeys.

Materials and Methods

siRNA. Givosiran, metabolite standards, and the internal standard were synthesized at Alnylam Pharmaceuticals (Cambridge, MA, USA) to ≥85% purity as described previously (Nair et al., 2014). The identities and purities of all oligonucleotides were confirmed by electrospray ionization mass spectroscopy and ion exchange high-performance liquid chromatography, respectively. The molecular weight of double-stranded givosiran is 16300.3 Da, with the antisense strand at 7563.8 Da and sense strand at 8736.5 Da.

In Vivo Studies. All animal procedures were conducted using protocols consistent with local, state, and federal regulations, as applicable, and approved by the Institutional Animal Care and Use Committee at Alnylam Pharmaceuticals. Givosiran was administered to male and female Sprague Dawley rats and cynomolgus monkeys via a single intravenous bolus or single and multiple subcutaneous injection at the dose levels defined in each study. Rats were approximately 7 to 12 weeks of age and 160 to 325 g at the initiation of dosing. Monkeys were 2 to 8 years of age and 2 to 6 kg at the initiation of dosing. The intravenous dose was 10 mg/kg in rats and monkeys, and the subcutaneous doses ranged from 1 to 10 mg/kg in rats and 1 to 30 mg/kg in monkeys. Plasma, urine, milk, feces, and other tissue (liver, kidney, etc.) samples were collected and stored frozen at approximately −70°C until analysis.

Metabolite Profiling and Quantitation by Liquid Chromatography Coupled with High Resolution Mass Spectrometry. Metabolite profiling of givosiran and quantitation of givosiran and its primary metabolite AS(N-1)3′ givosiran, a double-stranded metabolite formed by loss of one nucleotide from the 3′ end of the antisense strand, was performed by liquid chromatography coupled with high resolution mass spectrometry (LC-HRMS), similar to the methods described previously (Li et al., 2019; Liu et al., 2019). Briefly, plasma, urine, milk, fecal homogenates, and tissue homogenates were processed by solid phase extraction using a Clarity OTX 96-well plate (Phenomenex, Torrance, CA) according to the manufacturer's recommended protocol, and the extracted samples were analyzed by LC-HRMS. The mobile phases used were as follows: mobile phase A: H_2O/hexafluoropropanol/diisopropylethylamine (100:1:0.1, v/v/v) with 10 μM EDTA; mobile phase B: H_2O/acetonitrile/hexafluoropropanol/diisopropylethylamine(35:65:0.75:0.0375, v/v/v/v) with 10 μM EDTA. The column used was DNAPac RP column (4 μm, 50 × 2.1 mm; Thermo Fisher Scientific, Waltham, MA). Column temperature was set between 80°C and 90°C, and flow rate was 0.2 ml/min. For metabolite profiling of givosiran, the gradient started with 5% B, progressed to 25% B over 20 minutes, then increased to 70% B in 0.1 minute and was maintained for 1.9 minutes, and was then washed with 100% B for 2 minutes; the column was re-equilibrated with 5% B for 5 minutes. For the quantitation of givosiran and AS(N-1)3′ givosiran, the gradient started with 10% B, progressed to 40% B over 4 minutes, and then increased to 100% B in 0.1 minute and was maintained for 1.9 minutes; the column was then re-equilibrated with 10% B for 4 minutes. A Dionex UltiMate 3000 HPLC system (Thermo Fisher Scientific) in combination with an Accela Open Autosampler (Thermo Fisher Scientific) and a Q Exactive mass spectrometer (Thermo Fisher Scientific) was used for the LC-HRMS analysis. The oligonucleotides were analyzed in negative ionization mode. For the metabolite profiling experiments, the mass spectrometer was set at full scan mode. For the quantitation experiments, the mass spectrometer was set either at targeted selected ion monitoring mode or at parallel reaction monitoring mode.

In Vitro Metabolic Stability and Metabolite Profiling. The metabolic stability and metabolite profile of the sense and antisense strands of givosiran were evaluated in pooled serum (BioIVT, Westbury, NY) and liver S9 fractions (Sekisue XenoTech, Kansas City, KS) from C57BL/6 mouse, Sprague Dawley rat, cynomolgus monkey, and human. Givosiran (5 or 10 μM) was incubated with serum or liver S9 fractions at 37°C for up to 24 hours. Reactions were terminated by the addition of EDTA solution and frozen in liquid nitrogen. The resulting samples were lysed at room temperature in the presence of Clarity OTX lysis-loading buffer (Phenomenex), cleaned up by solid phase extraction, and analyzed by LC-HRMS methods as described above. The double-stranded givosiran was denatured under the LC-HRMS condition, and the antisense strand and sense strand were detected as separate chromatographic peaks by LC-HRMS. The percentage of strand remaining was calculated by dividing the peak area ratio for each strand to internal standard (an siRNA having different molecular weight from givosiran) at each time point by the value of the peak area ratio at time zero and multiplying by 100%, as shown below:

$$\text{Percent strand remaining} = \text{Peak Area Ratio}_{(\text{time point})} \div \text{Peak Area Ratio}_{(\text{time zero})} \times 100\%.$$

In Vitro Potency. Hep3B cells were transfected by adding 4.9 μl of optimized minimal essential medium plus 0.1 μl of Lipofectamine RNAiMAX Transfection Reagent per well (Invitrogen) to 5 μl of givosiran or AS(N-1)3′ givosiran per well into a 384-well plate. The plate was incubated at room temperature for 15 minutes, and then 40 μl of Eagle's minimum essential medium containing $\sim 5 \times 10^3$ cells was added to the mixture. Cells were incubated for 24 hours before RNA purification. ALAS1 gene reduction potential was evaluated at final concentrations of 10 and 0.1 nM for both givosiran and AS(N-1)3′ givosiran.

Pharmacokinetic Analysis. Noncompartmental PK parameter estimates were determined from individual concentration-time data, using Phoenix WinNonlin, version 7.0 (Certara USA, Princeton, NJ). C_{max} results were reported as observed values, and area under the plasma concentration-time curve from the time of dosing to the last measurable concentration (AUC_{last}) was estimated using the linear trapezoidal rule (linear interpolation). The apparent terminal elimination half-life ($t_{1/2}$) was calculated as $0.693/\lambda$, where λ is the first-order rate constant associated with the terminal portion of the concentration-time curve. Half-life was considered not reportable if there were fewer than three quantifiable concentration-time data points on the terminal phase (not including concentration-time points before C_{max}), the coefficient of determination (r^2) was less than 0.85, or $t_{1/2}$ was longer than the time of the last quantifiable sample. Mean givosiran and metabolite concentrations (and associated descriptive statistics, e.g., mean and S.D.) were calculated using Phoenix WinNonlin, version 7.0. Figures were created in GraphPad Prism version 7.03.

Plasma Protein Binding. Plasma protein binding (PPB) was analyzed by electrophoretic mobility shift assay (EMSA) as reported previously (Rocca et al., 2019). Briefly, givosiran was incubated at concentrations of 1.0, 5.0, 10, 25, and 50 μg/ml in K_2EDTA plasma (BioIVT) or PBS for 1 hour at 37°C. EMSA Gel Loading Solution (Thermo Fisher Scientific) was added to samples prior to separation on a 10% Tris/Borate/EDTA (TBE) Gel (Bio-Rad Laboratories, Hercules, CA). The gel was run on ice for 1 hour at 100 V followed by staining with SYBR Gold Nucleic Acid Gel Stain (Thermo Fisher Scientific) and washing with TBE (Bio-Rad Laboratories). Gel images were obtained and analyzed using the Gel Doc XR+ System with Image Laboratory version 5.2 (Bio-Rad Laboratories).

Free (unbound) givosiran was defined as the bands in the sample wells that did not shift relative to their PBS control wells. The intensity of the free givosiran band in the plasma lane was compared with the intensity of the PBS control band on the same gel to determine the percent free givosiran in the sample. The percent bound givosiran was determined by performing the following calculation: (percent bound) = 100 – (percent free).

Drug-Drug Interaction. Givosiran was evaluated for potential drug interaction involving cytochrome P450 (P450) isozymes (inhibition and induction) and drug transporters

(substrate and inhibition) as reported previously (Ramsden et al., 2019). Briefly, P450 direct and time-dependent inhibition potential of givosiran was evaluated using human liver microsomes with the appropriate substrate for each P450 isozyme at givosiran concentrations up to 600 μM (10 mg/ml). P450 induction potential was also evaluated using cryopreserved human hepatocytes from three different donors at givosiran concentrations up to 6.1 μM (100 μg/ml). Potential interaction of givosiran with known efflux and uptake transporters was tested using various membrane vesicles and transfected cell lines.

Results

Absorption

Givosiran Plasma Pharmacokinetics in Rats. The plasma PK of givosiran were evaluated after a single intravenous dose (10 mg/kg) and single subcutaneous administration with doses ranging from 1 to 10 mg/kg in male and female rats, and the plasma PK parameters are shown in Table 1. There were no apparent sex differences in the PK parameters in rats; therefore, the PK parameters presented are based on overall mean values generated by combining sexes. After a single intravenous dose of 10 mg/kg, the elimination from the plasma was rapid with an estimated $t_{1/2}$ of 0.2 hours. The mean total clearance (CL) and volume of distribution at steady state (V_{ss}) values were 870 ml/h per kg and 181 ml/kg, respectively. After a single subcutaneous administration, plasma exposure of givosiran [C_{max} and area under the curve (AUC)] increased with the dose over the dose range evaluated. The apparent plasma $t_{1/2}$ was consistent across subcutaneous doses (range 2 to 3 hours). The PK profile of givosiran was also evaluated in rats after weekly repeat subcutaneous doses at 1 mg/kg. Consistent with the short apparent $t_{1/2}$ of 2 to 3 hours in plasma, there was no evidence of accumulation in plasma after repeat dosing (data not shown).

A separate PK study in rats was conducted to determine the relative plasma exposure and PK profile of the primary metabolite, AS(N-1)3′ givosiran (loss of one nucleotide from the antisense strand 3′ end) after a single subcutaneous dose of givosiran at 10 mg/kg. Plasma C_{max} of givosiran and AS(N-1)3′ givosiran were 1.06 and 0.190 μg/ml, respectively. Plasma AUC_{last} of givosiran and AS(N-1)3′ givosiran were 3.00 and 0.626 hour·μg/ml, respectively. Plasma exposure of AS(N-1)3′ givosiran as assessed by AUC_{last} was approximately 21% of exposure of givosiran. After reaching C_{max}, givosiran and AS(N-1)3′ givosiran concentrations declined with the $t_{1/2}$ value of 3.0 and 8.2 hours, respectively (Table 2; Fig. 1).

Givosiran Plasma Pharmacokinetics in Monkeys. The plasma PK of givosiran was evaluated after a single intravenous dose (10 mg/kg) and single subcutaneous doses ranging from 1 to 10 mg/kg in male and female monkeys, and the plasma PK parameters are shown in Table 3. There were no apparent sex differences in the PK parameters in monkeys; therefore, the PK parameters presented are based on overall mean values generated by combining sexes. After a single intravenous dose of 10 mg/kg, the elimination from systemic circulation was rapid with an estimated $t_{1/2}$ of 0.2 hours. The mean CL and V_{ss} values were 340 ml/h per kg and 104 ml/kg, respectively. After a single subcutaneous administration, plasma exposure of givosiran (C_{max} and AUC_{last}) increased as the dose increased over the dose range tested. The apparent plasma $t_{1/2}$ was consistent across subcutaneous doses (approximately 3.5 hours). The PK profile of givosiran was also evaluated in monkeys after multiple weekly subcutaneous doses at 1 mg/kg (Table 3). There was no evidence of accumulation in plasma after weekly repeat dosing.

A separate PK study in monkeys was conducted to determine the relative plasma exposure and the PK of the primary metabolite, AS(N-1)3′ givosiran, after a single subcutaneous dose of givosiran at 30 mg/kg. The C_{max} of givosiran and AS(N-1)3′ givosiran in plasma were 2.42 and 1.67 μg/ml, respectively. Plasma AUC_{last} of givosiran and AS(N-1)3′ givosiran were 26.4 and 19.4 hour·μg/ml, respectively. Plasma exposure of AS(N-1)3′ givosiran as assessed by AUC_{last} was approximately 74% of exposure of givosiran. After reaching C_{max}, givosiran and AS(N-1)3′ givosiran concentrations declined with the $t_{1/2}$ values of 5.5 and 5.1 hours, respectively (Table 4; Fig. 2).

TABLE 1

Overall mean givosiran plasma pharmacokinetic parameters in rats after a single intravenous bolus or subcutaneous administration

	Intravenous	Subcutaneous		
	10 mg/kg	1 mg/kg	5 mg/kg	10 mg/kg
t_{max} (h)	—	0.3	0.4	1.1
C_{max} (μg/ml)	—	0.11	0.43	1.07
AUC_{last} (h·μg/ml)	11.8	0.15	1.29	2.79
$t_{1/2}$ (h)	0.2	2.1	2.7	2.7
V_{ss} (ml/kg)	181	—	—	—
CL (ml/h per kg)	870	—	—	—

Values represent the overall combined (male + female) mean. $n = 4$. —, not applicable; t_{max}, time to reach maximum concentration.

Distribution

Plasma Protein Binding. Conventional methodologies commonly used to determine PPB such as equilibrium dialysis and ultrafiltration were inadequate for new chemical modalities such as siRNAs because of extensive nonspecific binding to the membrane resulting in inaccurate measurement of PPB. Therefore, EMSA was used to determine the PPB of givosiran in mouse, rat, monkey, and human plasma (Rocca et al., 2019). For givosiran concentrations ranging from 1 to 50 μg/ml, the extent of plasma protein binding was concentration dependent, as shown in Table 5. In all species tested, the percentage of binding decreased as givosiran concentration increased. In general, PPB is similar across species. The mechanism of nonlinear PPB is likely due to saturation of binding at high concentrations. However, the mean plasma C_{max} of givosiran at steady state after subcutaneous administration of 2.5 mg/kg in humans is 0.321 μg/ml, which is well below the concentration where binding saturation was observed. Therefore, plasma protein binding is expected to remain relatively constant (∼90%) over the clinically relevant plasma concentrations.

Distribution in Rats. Givosiran is specifically designed for delivery to the liver through GalNAc moieties bound to the siRNA that direct hepatocyte-specific uptake of the siRNA via the ASGPR expressed on the cell surface of hepatocytes. Consistent with this design, givosiran predominantly distributed to the liver after the administration of a subcutaneous dose (Table 6). The liver-to-plasma AUC ratio was approximately 4500, and the $t_{1/2}$ in the liver was significantly longer (∼120 hours) than that in plasma. The liver exposure after a single subcutaneous dose of 10 mg/kg was significantly higher than that after intravenous dosing (Table 6, Fig. 3) indicating that liver uptake is more efficient after subcutaneous administration. More efficient liver uptake after a subcutaneous dose is likely due to a gradual increase (rather than a sharp increase after intravenous dose) in plasma concentration, potentially avoiding saturation of ASGPR-mediated hepatic uptake.

TABLE 2

Mean ± S.D. givosiran and AS(N-1)3′ givosiran plasma pharmacokinetic parameters in rats after a single subcutaneous dose (10 mg/kg)

	Givosiran ($n = 4$)	AS(N-1)3′ givosiran ($n = 4$)
C_{max} (μg/ml)	1.06 ± 0.414	0.190 ± 0.0701
AUC_{last} (h·μg/ml)	3.00 ± 0.458	0.626 ± 0.132
$t_{1/2}$ (h)	3.0	8.2

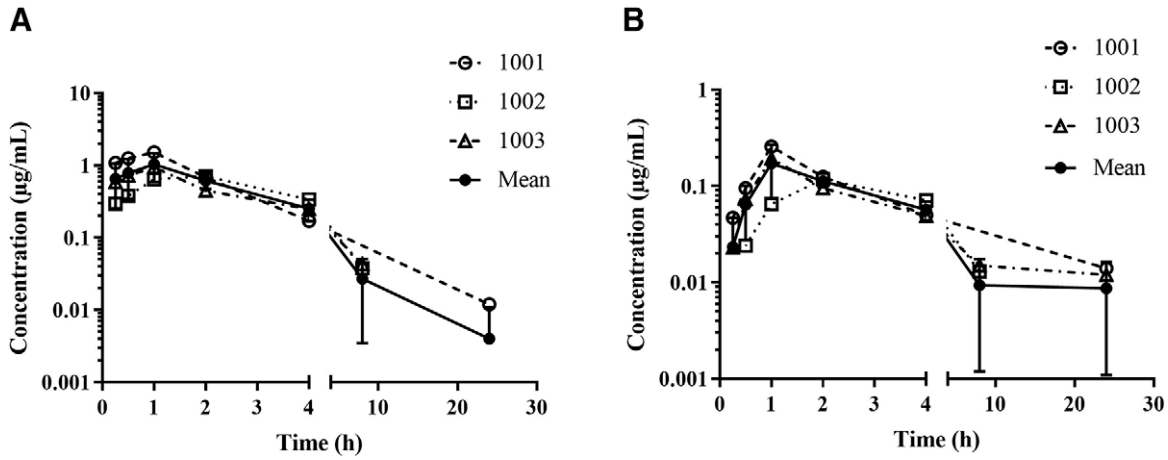

Fig. 1. Individual and mean (± S.D.) plasma concentration-time profiles of givosiran (A) and AS(N-1)3′ givosiran (B) in rats after a single subcutaneous administration of givosiran (10 mg/kg). Plasma C_{max} values of givosiran and AS(N-1)3′ givosiran were 1.06 and 0.190 µg/ml, respectively. Plasma AUC_{last} values of givosiran and AS(N-1)3′ givosiran were 3.00 and 0.626 hour·µg/ml, respectively. Plasma exposure of AS(N-1)3′ givosiran as assessed by AUC_{last} was approximately 21% of exposure of givosiran. After reaching C_{max}, givosiran and AS(N-1)3′ givosiran concentrations declined with the $t_{1/2}$ value of 3.0 and 8.2 hours, respectively. Note: Error bars indicate S.D. Lower limit of quantitation = 10 ng/ml. Below–lower limit of quantitation concentrations were treated as 0. Results are presented for individual animals (open symbols) and as mean (closed circles; n = 3).

TABLE 3

Overall mean givosiran plasma pharmacokinetic parameters in monkey plasma after administration of a single intravenous bolus or single or multiple subcutaneous dose

	Intravenous	Subcutaneous			
	Single dose	Single dose			Multiple dose[a]
	10 mg/kg	1 mg/kg	5 mg/kg	10 mg/kg	1 mg/kg
t_{max} (h)	—	1.1	2.4	1.7	1.5
C_{max} (µg/ml)	—	0.133	0.830	2.14	0.136
AUC_{last} (h·µg/ml)	30.5	0.324	4.65	11.2	0.379
$t_{1/2}$ (h)	0.2	3.2	3.5	3.5	2.8
CL (ml/h per kg)	340	—	—	—	—
V_{ss} (ml/kg)	104	—	—	—	—

Values represent the overall combined (male + female) mean. n = 6. —, not applicable; t_{max}, time to reach maximum concentration; $V_{s,}$ volume of distribution at steady state.
[a]Monkeys were administered givosiran once weekly for a total of eight doses. PK values were determined on day 50.

TABLE 4

Mean ± S.D. givosiran and AS(N-1)3′ givosiran plasma pharmacokinetic parameters in monkeys after a single subcutaneous dose (30 mg/kg)

	Givosiran (n = 4)	AS(N-1)3′ givosiran (n = 4)
C_{max} (µg/ml)	2.42 ± 0.664	1.67 ± 0.0551
AUC_{last} (h·µg/ml)	26.4 ± 4.96	19.4 ± 4.28
$t_{1/2}$ (h)	5.5 ± 1.7	5.1 ± 2.1

Consequently, higher plasma concentrations after an intravenous bolus dose resulted in higher concentrations of givosiran in the kidneys where distribution of givosiran from the plasma is likely to be passive diffusion (i.e., no ASGPR-mediated uptake). In fact, the distribution of givosiran to liver and kidney was comparable after intravenous administration (10 mg/kg), whereas the distribution of givosiran based on C_{max} and AUC_{last} to the liver was substantially higher (~10-fold and ~4-fold, respectively) than to the kidney after subcutaneous administration (Table 6, Fig. 4).

Markedly lower concentrations of givosiran (100–800-fold over liver) were observed in adrenal, heart, lung, spleen, thyroid, thymus, pancreas, jejunum, and testes. Givosiran was not detected in the brain.

After weekly subcutaneous dosing (total of 8 doses) of 1 mg/kg, C_{max} and AUC_{last} of givosiran in the liver were 25.9 µg/g and 1290 hour·µg/g, respectively, and there was no evidence of accumulation. However, the C_{max} and AUC_{last} of givosiran in the kidney were 5.45 µg/g and 1190 hour·µg/g, respectively, and the exposure was three to four times higher compared with the dose normalized exposure after a single dose, indicating that givosiran accumulated in the kidney after repeated weekly subcutaneous doses.

Distribution in Monkeys. As observed in rats, givosiran extensively distributed to the liver of monkeys, where concentrations were measurable up to 672 hours after a single intravenous dose (10 mg/kg). After a single subcutaneous dose (1, 5, or 10 mg/kg), givosiran was detectable in the liver up to 672 to 1008 hours postdose with maximum liver concentrations observed between 8 to 24 hours postdose. The AUC_{last} in the liver was approximately 7-fold higher after a single subcutaneous dose of 10 mg/kg than after the same dose administered intravenously (Table 7; Fig. 5), indicating that liver uptake is more efficient after subcutaneous administration compared with intravenous administration. The liver-to-plasma AUC ratio was approximately 2500, and the $t_{1/2}$ in the liver was significantly longer (~146 hours) than that in plasma.

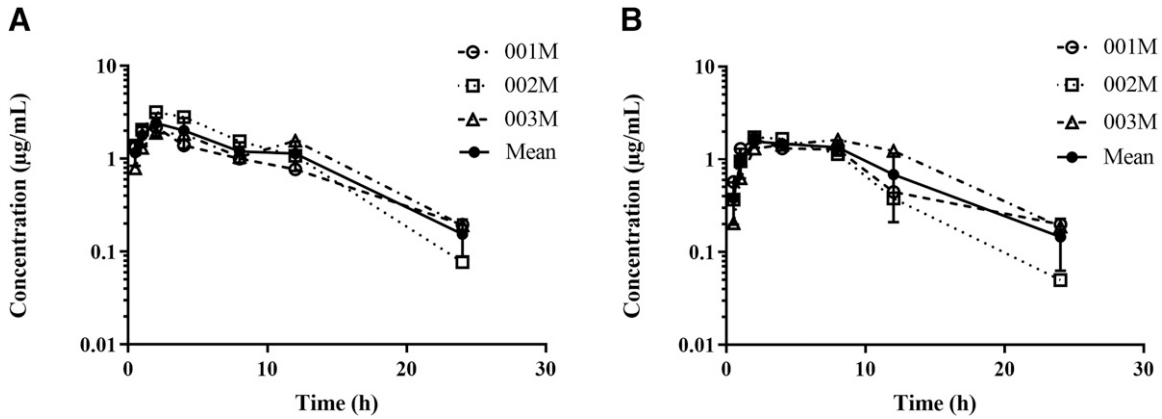

Fig. 2. Individual and mean (± S.D.) plasma concentration-time profiles of givosiran (A) and AS(N-1)3′ givosiran (B) in male monkeys after a single subcutaneous administration of givosiran (30 mg/kg). The C_{max} values of givosiran and AS(N-1)3′ givosiran in plasma were 2.42 and 1.67 µg/ml, respectively. Plasma AUC_{last} values of givosiran and AS(N-1)3′ givosiran were 26.4 and 19.4 hour·µg/ml, respectively. Plasma exposure of AS(N-1)3′ givosiran as assessed by AUC_{last} was approximately 74% of exposure of givosiran. After reaching C_{max}, givosiran and AS(N-1)3′ givosiran concentrations declined with the $t_{1/2}$ values of 5.5 and 5.1 hours, respectively. Note: Error bars indicate S.D. Lower limit of quantitation = 10 ng/ml. Results are presented for individual animals (open symbols) and mean (closed circles; n = 3).

TABLE 5

Plasma protein binding of givosiran

	Mean percent plasma protein binding by concentration				
	1.0 µg/ml	5.0 µg/ml	10 µg/ml	25 µg/ml	50 µg/ml
Mouse	91.3	79.8	61.8	38.1	10.1
Rat	93.1	89.0	78.6	51.6	27.5
Monkey	89.5	82.7	69.9	43.9	25.9
Human	91.8	83.4	71.4	39.2	21.1

TABLE 6

Overall mean givosiran liver and kidney pharmacokinetics in rats after a single intravenous bolus or subcutaneous dose (10 mg/kg)

	Liver		Kidney	
	Intravenous	Subcutaneous	Intravenous	Subcutaneous
t_{max} (h)	2.1	4.0	0.3	6.0
C_{max} (µg/g)	102	208	81.0	19.0
AUC_{last} (h·µg/g)	5390	12,600	5440	3190
$t_{1/2}$ (h)	55	120	119	172

t_{max}, time to reach maximum concentration. Values represent results for overall combined (male + female) mean. n = 4.

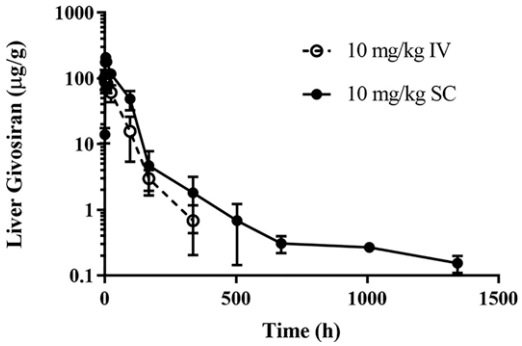

Fig. 3. Mean liver concentration-time profiles of givosiran in rats after an intravenous bolus and subcutaneous administration (10 mg/kg). Liver AUC_{last} values of givosiran were 5390 hour·µg/g and 12,600 hour·µg/g after a single intravenous or subcutaneous dose, respectively. The liver exposure after a single subcutaneous dose of 10 mg/kg was significantly higher than that after intravenous dosing, indicating that liver uptake is more efficient after subcutaneous administration. IV, intravenous; SC, subcutaneous. Error bars indicate S.D. n = 4 animals per group per time point.

Mean C_{max} and AUC_{last} values increased approximately dose proportionally across the dose range tested. After eight weekly subcutaneous doses of 1 mg/kg, C_{max} and AUC were 16.9 µg/g and 3340 hour·µg/g, respectively, suggesting minimal accumulation in the liver with repeat dosing. The $t_{1/2}$ was consistent across doses and regimen, indicating no dose- or time-dependent PK.

Metabolism

In Vitro Metabolic Stability of Givosiran in Serum and Liver S9 Fractions. The in vitro metabolic stability of givosiran was evaluated in pooled serum and liver S9 fractions obtained from C57BL/6 mouse, rat, monkey, and human, at a concentration of 5 µM. The reaction mixtures were incubated at 37°C for up to 24 hours for both serum and liver S9 fractions.

Stability of givosiran in serum was generally similar across species, with the sense strand being more stable than the antisense strand. After 24 hours of incubation of givosiran in mouse, rat, monkey, or human serum, the percentage of antisense strand remaining was approximately 75%, 59%, 63%, and 89%, respectively; the percentage of sense strand remaining was approximately 95%, 95%, 100%, and 95%, respectively.

When mouse, rat, monkey, or human liver S9 fraction was incubated with givosiran (5 µM) for 24 hours, the stability profiles for the four species exhibited the rank order from most to least stable of mouse > monkey > human > rat, for both strands. The percentage of antisense strand remaining after 24 hours of incubation for mouse, monkey, human, and rat was approximately 103%, 68%, 49%, and 36%, respectively, and the percentage of sense strand remaining was approximately 102%, 88%, 65%, and 64%, respectively.

A separate in vitro study was conducted in human liver S9 fraction with and without NADPH to determine if givosiran was metabolized by drug metabolizing enzymes requiring NADPH as a cofactor (e.g., P450s). Givosiran was incubated at a concentration of 10 µM in human liver S9 fraction (total protein concentration of 1 mg/ml) with and without NADPH (1 mM) for 1 hour at 37°C. Both sense and

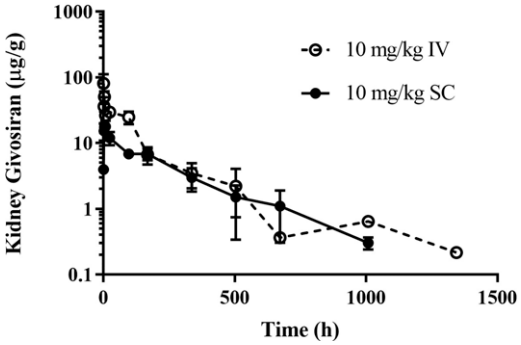

Fig. 4. Mean kidney concentration versus time profiles of givosiran in rats after an intravenous bolus and subcutaneous administration (10 mg/kg). Kidney AUC_{last} values of givosiran were 5440 hour·µg/g and 3190 hour·µg/g after a single intravenous or subcutaneous dose, respectively. Higher plasma concentrations after an intravenous bolus dose resulted in higher concentrations of givosiran in the kidneys where distribution of givosiran from the plasma is likely to be passive diffusion (i.e., no ASGPR-mediated uptake). IV, intravenous; SC, subcutaneous. Error bars indicate S.D. $n = 4$ animals per group per time point.

TABLE 7

Overall mean givosiran pharmacokinetics in monkey livers after a single intravenous bolus or subcutaneous dose

	Intravenous bolus	Subcutaneous dose		
	10 mg/kg	1 mg/kg	5 mg/kg	10 mg/kg
t_{max} (h)	8.0	16.0	24.0	8.0
C_{max} (µg/g)	41.5	28.3	154	204
AUC_{last} (h·µg/g)	4220	2540	17,900	28,500
$t_{1/2}$ (h)	164	211	167	146

t_{max}, time to reach maximum concentration. Values represent the overall combined (male + female) mean. $n = 2$.

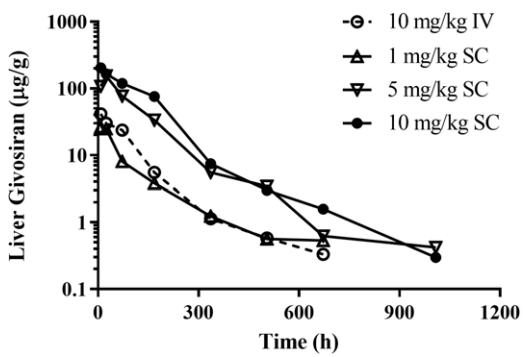

Fig. 5. Mean liver concentration-time profiles of givosiran in monkeys after an intravenous bolus (10 mg/kg) and subcutaneous administration of givosiran (1–10 mg/kg). After a single subcutaneous dose (1, 5, or 10 mg/kg), givosiran was detectable in the liver up to 672–1008 hours postdose with maximum liver concentrations observed between 8 and 24 hours postdose. The AUC_{last} in the liver was 4220 hour·µg/g and 28,500 hour·µg/g, respectively, after a single intravenous or subcutaneous dose of 10 mg/kg. The ~7-fold higher liver AUC_{last} after a single subcutaneous dose than after the same dose administered intravenously, indicates that liver uptake is more efficient after subcutaneous administration compared with intravenous administration. IV, intravenous; SC, subcutaneous. $n = 2$ animals per group per time point.

antisense strands of givosiran were stable, and no change was observed with and without NADPH, suggesting that P450 isozymes are not involved in the metabolism of givosiran (Table 8). Verapamil (5 µM) was used as a positive control to confirm the integrity of the human liver S9 fraction used.

Metabolite Profiling of the Antisense Strand. Metabolite profiling was conducted with serum samples obtained from in vitro stability studies and plasma samples collected from in vivo PK studies. Either in serum (mouse, rat, monkey, and human) or in plasma (rat and monkey), givosiran was metabolized to form a primary metabolite, AS(N-1)3′ givosiran or AS(N-1)5′ givosiran (metabolite with loss of one nucleotide from the 5′ end of the antisense strand). Mass spectra showed that metabolites, AS(N-1)3′ givosiran and AS(N-1)5′ givosiran, have the exact same mass and were presumably formed by the loss of a uridine monophosphate nucleotide from either the 3′ or 5′ end of the antisense strand. The two metabolites have the same high-performance liquid chromatography retention time as well and thus cannot be differentiated by a liquid chromatography–mass spectrometry method. A specific liquid chromatography–tandem mass spectrometry method was developed to differentiate AS(N-1)3′ givosiran and AS(N-1)5′ givosiran by monitoring unique fragment ions for AS(N-1)3′ at *m/z* 604.1032 (b_2 fragment ion) and at *m/z* 632.1188 (y_2 fragment ion) for AS(N-1)5′. Quantitation of AS(N-1)3′ and AS(N-1)5′ metabolites in plasma and liver samples (rat and monkey) using this liquid chromatography–tandem mass spectrometry method confirmed that the primary metabolite was AS(N-1)3′ givosiran; AS(N-1)5′ givosiran was not detected in any samples from in vivo studies.

Human plasma and urine samples obtained from two patients of the phase 1 trial (Agarwal et al., 2020) were also analyzed to identify potential metabolite(s). As observed with the rat and monkey plasma metabolite profile, AS(N-1)3′ givosiran was the main circulating metabolite, and no other metabolite(s) were detected in human plasma. Consistent with the finding in plasma, AS(N-1)3′ givosiran was the only metabolite detected in the urine samples of these two patients. These results indicated that the metabolite profile of the antisense strand of givosiran was similar across all species tested.

The in vitro potency of givosiran and AS(N-1)3′ givosiran was evaluated by transfection in human hepatocellular carcinoma cell line 3B cells. At 10 nM siRNA concentration, the *ALAS1* mRNA remaining relative to negative control is 16.4% for givosiran and 10.3% for AS(N-1)3′ givosiran. At 0.1 nM siRNA concentration, the *ALAS1* mRNA remaining is 69.1% for givosiran and 52.0% for AS(N-1)3′ givosiran. The retention of AS(N-1)3′ givosiran pharmacological activity in vitro suggests that it is likely, to the extent that it is present, to contribute to observed in vivo pharmacology.

Preferential formation of AS(N-1)3′ givosiran over AS(N-1)5′ givosiran may be due to some steric hindrance caused by the presence of the GalNAc ligand at the 3′ end of the sense strand (i.e., close to the 5′ end of antisense strand; Fig. 6). Such steric hindrance may prevent exonuclease-mediated metabolism at the 3′ end of the sense and the 5′ end of the complementary antisense strand. In contrast to the 5′ end of the antisense strand, the 3′ end of the antisense strand is single stranded and therefore more susceptible to degradation by 3′ exonucleases.

In vitro metabolite profiling conducted in liver S9 fraction from mouse, rat, monkey, and human identified that the givosiran antisense strand was metabolized to form AS(N-3)5′ givosiran (metabolite with loss of three nucleotides from the 5′ end of antisense strand) and AS(N-1)3′ givosiran as two primary metabolites, with the AS(N-3)5′ givosiran being the most abundant. The metabolite profile was consistent among all the species tested. However, liver samples collected in the rat and monkey PK studies showed that givosiran antisense strand was metabolized to form a primary metabolite, AS(N-1)3′ givosiran. In addition to AS(N-1)3′ givosiran, other minor metabolites (products after cleavage of nucleotides by exo- and endonucleases) were detectable (Fig. 6).

Metabolite Profiling of the Sense Strand. Either in serum (mouse, rat, monkey, and human) or in plasma (rat and monkey), the givosiran

TABLE 8

In vitro metabolic stability of givosiran in human liver S9 fraction with and without cofactor (NADPH)

	Percentage remaining (mean ± S.D.) (n = 3)					
	Givosiran (without NADPH)			Givosiran (with NADPH)		
Time	Antisense	Sense	Verapamil	Antisense	Sense	Verapamil
0 h	100 ± 2.66	100 ± 2.94	100 ± 7.81	100 ± 3.53	100 ± 7.49	100 ± 7.01
1 h	104 ± 2.28	97 ± 3.44	88 ± 5.71	98 ± 1.53	96 ± 4.61	33 ± 5.42

sense strand was minimally metabolized primarily generating a metabolite corresponding to the loss of 1 GalNAc group from the triantennary ligand at the 3′ end (Fig. 6). Similar to the finding in rat and monkey plasma, givosiran with the loss of one or three GalNAc groups from the sense strand was also detected in plasma and urine from two human patients.

Metabolite profiling of in vitro liver S9 fractions (mouse, rat, monkey, and human) and in vivo rat and monkey liver samples showed that the primary putative metabolites of the givosiran sense strand were generated by the loss of one, two, or all three GalNAc moieties at the 3′ end. Loss of GalNAc was evident at the earliest time point of 2 hours, with no intact senses strand remaining by 24 hours in liver samples.

The collective data characterizing the metabolism of the antisense and sense strands demonstrated that overall the in vitro metabolite profiles for givosiran were comparable to those profiles observed from the in vivo study samples, and the overall metabolite profiles of givosiran were similar across all species tested, including human.

Excretion

Excretion in Rats. Givosiran was quantitated in pooled urine and fecal samples collected over a period of 168 hours after a single subcutaneous administration of 10 mg/kg in rats. Approximately 10% of the total administered dose was excreted as givosiran in urine within the first 168 hours (mostly within the first 24 hours) in rats. A negligible amount of givosiran (∼0.1% of the total administered dose) was recovered in feces collected over 48 hours postdose. Biliary excretion of givosiran was also evaluated in bile-duct cannulated rats after a single subcutaneous dose of 10 mg/kg, and approximately 6% of the dose was recovered as unchanged givosiran. Excretion of givosiran in milk was negligible as the concentration of givosiran was not measurable in the milk collected from female rats treated with multiple subcutaneous doses up to 30 mg/kg in a developmental and perinatal/postnatal reproduction study. Therefore, excretion is a minor route of overall elimination of givosiran after subcutaneous administration in rats.

Excretion in Monkeys. Givosiran was quantitated in pooled urine and fecal samples collected over a period of 168 hours after a single administration of 10 mg/kg in monkeys. Approximately 16% of the administered dose was recovered as givosiran in urine within the first 168 hours in monkeys. The majority of excretion occurred within the first 24 hours. Givosiran was not detectable in any of the pooled fecal samples collected. Therefore, consistent with observations in rats, excretion (renal and fecal) is a minor route of overall elimination of givosiran after a subcutaneous administration in monkeys.

Drug-Drug Interaction. The drug-drug interaction (DDI) potential of givosiran was examined using various in vitro assays (e.g., human liver microsomes, human hepatocytes, transfected cell lines, and membrane vesicles) based on regulatory guidance. Experimental details and results of these studies were previously reported in a recent review publication (Ramsden et al., 2019). As a part of ADME properties, a brief summary of the study outcomes is described here. Givosiran was not a substrate of P450 isozymes as demonstrated by a lack of effect of NADPH on the metabolic stability of givosiran in human liver S9 fraction. Givosiran was not a direct or time dependent inhibitor of P450 isozymes (CYP1A2, CYP2B6, CYP2C8, CYP2C9, CYP2C19, CYP2D6, or CYP3A4/5) or an inducer of P450 isozymes (CYP1A2, CYP2B6, and CYP3A4).

Givosiran was not a substrate/inhibitor of the following human ATP-binding cassettes and solute carrier transporters: breast cancer resistance protein, bile salt export pump, organic anion transporting polypeptides (OATP1B1 and OATP1B3), organic anion transporters (OAT1 and OAT3), organic cation transporters (OCT1 and OCT2), and multidrug and toxin extrusion proteins (MATE1 and MATE2 K). However, P-glycoprotein exhibited 23% and 69% inhibition at givosiran concentrations of 1 and 10 μM, respectively, indicating that the IC_{50} is likely to be between 1 and 10 μM. The mean total plasma C_{max} of givosiran at steady state after subcutaneous administration of 2.5 mg/kg in humans is below 20 nM (Agarwal et al., 2020), and the unbound plasma C_{max} is about ∼2 nM using 90% plasma protein binding at that concentration. To be conservative, IC_{50} can be assumed to be closer to 1 μM. Therefore, unbound $[I]/IC_{50}$ is ∼0.002 (i.e., 2 nM/1000 nM), and a clinically relevant drug interaction involving P-glycoprotein is not expected. The DDI potential of AS(N-1)3′ givosiran was not evaluated separately. However, based on the similar physicochemical properties, the DDI potential is likely to be similar to givosiran. Taken together, givosiran has a low potential of mediating a DDI involving P450 isozymes and drug transporters.

Discussion

Givosiran is an approved RNAi therapeutic for the treatment of AHP in adults and adolescents aged 12 years or older. The recommended givosiran dose is 2.5 mg/kg once monthly by subcutaneous injection. Givosiran is specifically designed for delivery to the liver through conjugation of a carbohydrate ligand (GalNAc) to the siRNA to direct hepatocyte-specific uptake of siRNA via the ASGPR, which is expressed on the cell surface of hepatocytes. The PK and ADME properties of givosiran were evaluated in a variety of in vitro and nonclinical in vivo studies to support clinical development of givosiran.

After subcutaneous administration at pharmacologic doses ranging from 1 to 10 mg/kg, plasma exposure (C_{max} and AUC) was approximately dose proportional in rats and monkeys demonstrating that givosiran exhibited linear PK at pharmacologically relevant doses. Elimination of givosiran was rapid after intravenous administration with a mean $t_{1/2}$ of approximately 0.2 hours in both species after a single 10 mg/kg dose. The mean $t_{1/2}$ was longer with subcutaneous administration (approximately 2.7 hours in rats and 3.5 hours in monkeys) compared with intravenous administration. The longer $t_{1/2}$ after subcutaneous administration is likely due to flip-flop kinetics in which the observed $t_{1/2}$ reflects the rate of absorption rather than the rate of elimination in the systemic circulation. The plasma exposure of givosiran is predominantly driven by liver uptake via the ASGPR, which is highly expressed in hepatocytes. This makes evaluation of bioavailability of givosiran difficult due to transient saturation of ASGPR by the high circulating concentrations of givosiran after intravenous administration. This leads to

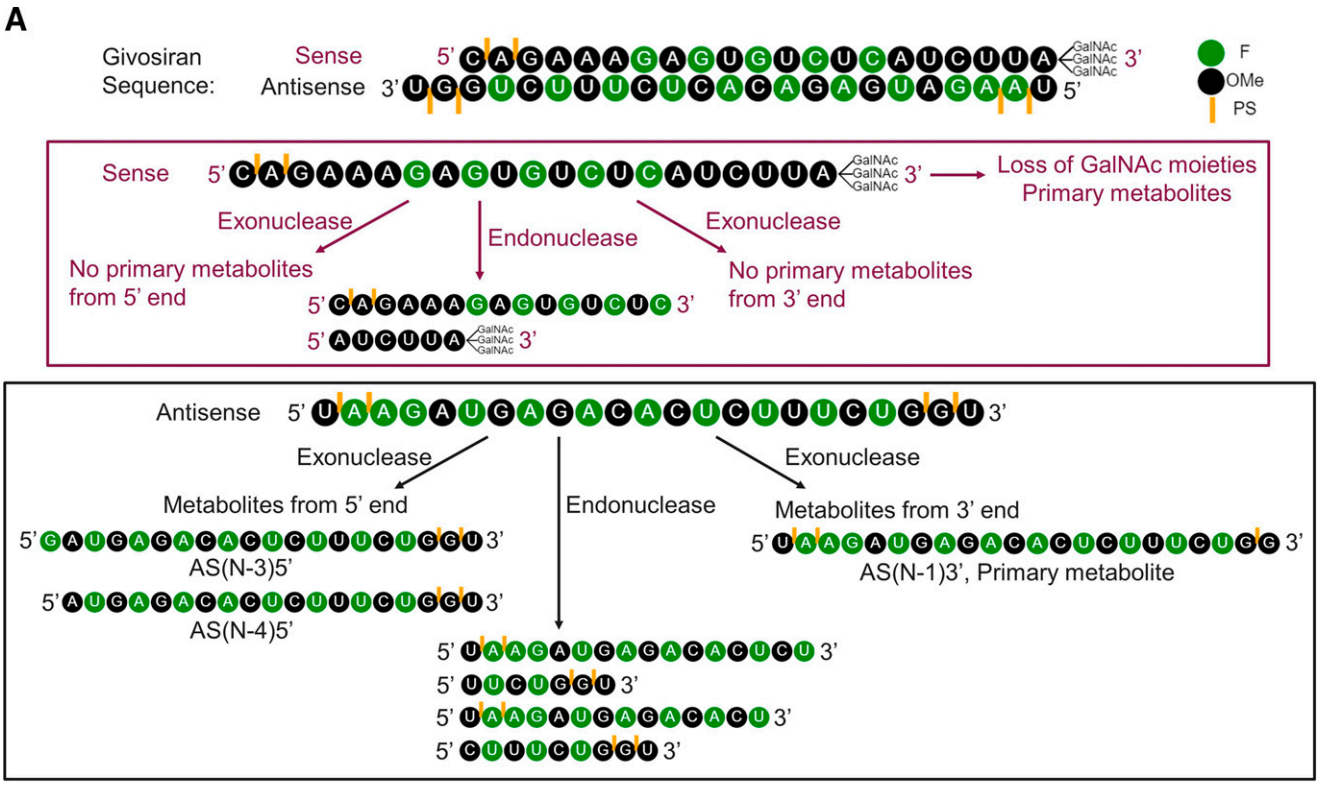

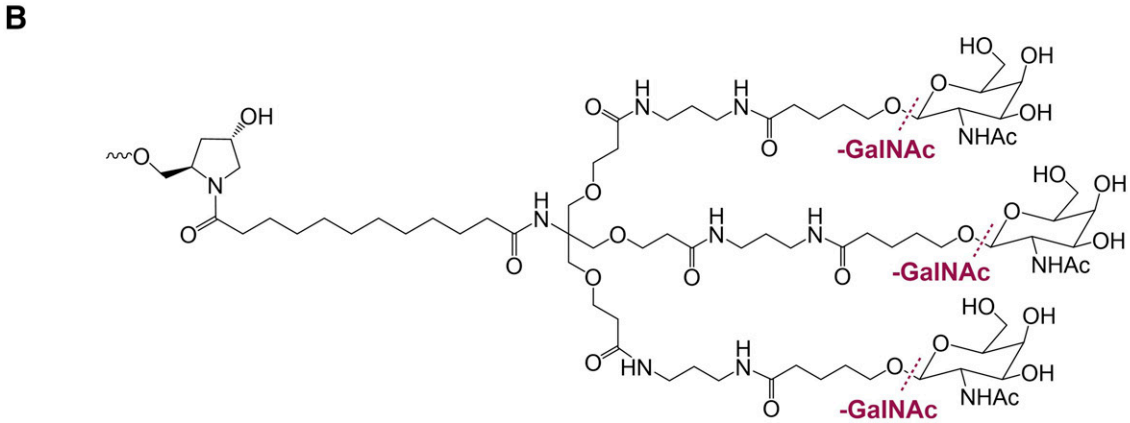

Fig. 6. Metabolism of givosiran. (A) Proposed biotransformation pathway of givosiran. (B) Chemical structure and cleavage sites of the metabolites of the triantennary GalNAc ligand of givosiran. Metabolite profiling was conducted with serum samples obtained from in vitro stability studies and plasma samples collected from in vivo PK studies. Either in serum or in plasma, givosiran was metabolized to form a primary metabolite, AS(N-1)3′ givosiran. Liver samples collected in the rat and monkey PK studies showed that givosiran antisense strand was metabolized to form a primary metabolite, AS(N-1)3′ givosiran. In addition to AS (N-1)3′ givosiran, other minor metabolites (products after cleavage of nucleotides by exo- and endonucleases) were detectable. Either in serum or in plasma, the givosiran sense strand was minimally metabolized primarily generating a metabolite corresponding to the loss of one GalNAc group from the triantennary ligand at the 3′ end. Metabolite profiling of in vitro liver S9 fractions and in vivo rat and monkey liver samples showed that the primary putative metabolites of the givosiran sense strand were generated by the loss of one, two, or all three GalNAc moieties at the 3′ end. All metabolites listed are double-stranded RNAs. Note: Black circles represent 2′-*O*-methyl (OMe)–modified nucleotides; green circles represent 2′-fluoro (F)–modified nucleotides; orange lines represent phosphorothioate (PS) bonds.

underestimation of subcutaneous bioavailability since much lower peak plasma concentrations after subcutaneous dosing do not saturate ASGPR and result in much lower plasma AUC values. The multiple dose plasma PK was consistent with single-dose data, and there was no evidence of accumulation in both rats and monkeys. Overall, these PK properties of givosiran in rats and monkeys indicate no time or dose dependence after pharmacological subcutaneous doses.

As expected, givosiran predominantly distributed to the liver via ASGPR-mediated hepatic uptake. The exposure of givosiran in the liver was significantly higher after subcutaneous administration than that after intravenous administration, indicating that liver uptake of givosiran is more efficient after subcutaneous administration. This is likely due to a more gradual increase in plasma concentration rather than a sharp increase after intravenous dose, potentially avoiding saturation of ASGPR-mediated hepatic uptake. This observation indirectly suggests

that the bioavailability of givosiran after subcutaneous administration is complete. Compared with all other tissue concentrations after a subcutaneous dose, kidney had the second highest concentration after liver. The liver-to-kidney exposure (AUC) ratio of givosiran was approximately 4-fold after subcutaneous administration of 10 mg/kg. Concentrations of givosiran in adrenal, heart, lung, spleen, thyroid, thymus, pancreas, jejunum, and testes were markedly (100–800-fold) lower than in liver. The liver-to-plasma AUC ratio was approximately 4500 and 2500 in rats and monkeys, respectively, and the $t_{1/2}$ in the liver was significantly longer (~120 and 146 hours) than that in plasma in rats and monkeys, respectively. Prolonged residence time in the target tissue (i.e., liver) is consistent with the observed duration of action in rats and monkeys. Givosiran was not detected in the brain and not expected to produce pharmacological effects in the central nervous system.

Givosiran antisense strand was metabolized by nucleases to form one primary active metabolite, AS(N-1)3′ givosiran in serum or plasma. In addition to AS(N-1)3′ givosiran, AS(N-3)5′ givosiran was formed in liver S9 fraction. However, only AS(N-1)3′ givosiran was detected in liver obtained from in vivo rat and monkey studies. The major putative metabolites of givosiran sense strand were generated by the loss of 1, 2, or all 3 GalNAc moieties at the 3′ end.

AS(N-1)3′ givosiran was the only circulating active metabolite in the plasma of rats, monkeys, and humans after subcutaneous administration. Relative to givosiran, the steady-state AUC exposure of AS(N-1)3′ givosiran in human plasma is approximately 49% after subcutaneous administration of 2.5 mg/kg givosiran once every month. The systemic exposure of AS(N-1)3′ givosiran after subcutaneous administration of givosiran was 21% and 73% relative to givosiran exposure in rats (10 mg/kg) and monkeys (30 mg/kg), respectively. Although not specifically measured, the plasma exposure to AS(N-1)3′ givosiran in chronic rat and monkey toxicology studies was expected to substantially exceed human exposure at the clinically intended dose. Therefore, safety of AS(N-1)3′ givosiran was adequately evaluated in the chronic rat and monkey toxicology studies.

The collective data characterizing the metabolism of the antisense and sense strands demonstrated that the in vitro metabolite profiles for givosiran were comparable to those profiles observed from the in vivo study samples, and the overall metabolite profiles of givosiran were similar across all species tested including human.

The renal and fecal excretion properties of givosiran were evaluated up to 168 hours after dosing after a single subcutaneous dose of 10 mg/kg in rats and monkeys. Approximately 10% of the administered dose was excreted as givosiran in urine in rats. Similar to observations in rats, 16% of the administered dose was excreted as givosiran in urine in monkeys. Fecal excretion of givosiran was only 0.1% of the administered dose in rats, and no givosiran was detected in monkey feces. Excretion of givosiran in milk was negligible in lactating female rats treated with multiple subcutaneous doses up to 30 mg/kg.

In summary, the PK and ADME properties of givosiran have been characterized in vitro and in vivo. Givosiran shows similar patterns of PK and ADME properties across the nonclinical species tested in vivo and across human and animal matrices in vitro. Collective data demonstrated that the subcutaneous administration of givosiran results in adequate exposure of the siRNA to the intended target organ (liver). Overall, the PK and ADME studies provide support for the interpretation of toxicology studies, help characterize the disposition of givosiran in humans at the dosing regimen of 2.5 mg/kg once monthly, and support the clinical use of givosiran for the treatment of acute hepatic porphyria.

Acknowledgments

The authors thank the previous employees, contract research organizations, executive management, and patients for their support of the studies.

Authorship Contributions

Participated in research design: Li, Liu, X. Zhang, Clausen, Xu, Smith, Wu, Chong.

Conducted experiments: Li, Liu, Tran, Arciprete, Wang, Rocca, Guan.

Performed data analysis: Li, Liu, X. Zhang, Tran, Arciprete, Wang, Rocca.

Wrote or contributed to the writing of the manuscript: Li, Liu, X. Zhang, Clausen, G. Zhang, Najarian, Wu, Chong.

References

Agarwal S, Simon AR, Goel V, Habtemariam BA, Clausen VA, Kim JB, and Robbie GJ (2020) Pharmacokinetics and pharmacodynamics of the small interfering ribonucleic acid, givosiran, in patients with acute hepatic porphyria. *Clin Pharmacol Ther* **108**:63–72.

Akinc A, Maier MA, Manoharan M, Fitzgerald K, Jayaraman M, Barros S, Ansell S, Du X, Hope MJ, Madden TD et al. (2019) The Onpattro story and the clinical translation of nanomedicines containing nucleic acid-based drugs. *Nat Nanotechnol* **14**:1084–1087.

Balwani M and Desnick RJ (2012) The porphyrias: advances in diagnosis and treatment. *Blood* **120**:4496–4504.

Balwani M, Sardh E, Ventura P, Peiró PA, Rees DC, Stölzel U, Bissell DM, Bonkovsky HL, Windyga J, Anderson KE et al.; ENVISION Investigators (2020) Phase 3 trial of RNAi therapeutic givosiran for acute intermittent porphyria. *N Engl J Med* **382**:2289–2301.

Bissell DM and Wang B (2015) Acute hepatic porphyria. *J Clin Transl Hepatol* **3**:17–26.

Chan A, Liebow A, Yasuda M, Gan L, Racie T, Maier M, Kuchimanchi S, Foster D, Milstein S, Charisse K et al. (2015) Preclinical development of a subcutaneous ALAS1 RNAi therapeutic for treatment of hepatic porphyrias using circulating RNA quantification. *Mol Ther Nucleic Acids* **4**:e263.

Foster DJ, Brown CR, Shaikh S, Trapp C, Schlegel MK, Qian K, Sehgal A, Rajeev KG, Jadhav V, Manoharan M et al. (2018) Advanced siRNA designs further improve in vivo performance of GalNAc-siRNA conjugates. *Mol Ther* **26**:708–717.

Hu B, Zhong L, Weng Y, Peng L, Huang Y, Zhao Y, and Liang XJ (2020) Therapeutic siRNA: state of the art. *Signal Transduct Target Ther* **5**:101.

Humphreys SC, Thayer MB, Campbell J, Chen WLK, Adams D, Lade JM, and Rock BM (2020) Emerging siRNA design principles and consequences for biotransformation and disposition in drug development. *J Med Chem* **63**:6407–6422.

Li J, Liu J, Enders J, Arciprete M, Tran C, Aluri K, Guan LH, O'Shea J, Bisbe A, Charissé K et al. (2019) Discovery of a novel deaminated metabolite of a single-stranded oligonucleotide in vivo by mass spectrometry. *Bioanalysis* **11**:1955–1965.

Liu J, Carmell MA, Rivas FV, Marsden CG, Thomson JM, Song JJ, Hammond SM, Joshua-Tor L, and Hannon GJ (2004) Argonaute2 is the catalytic engine of mammalian RNAi. *Science* **305**:1437–1441.

Liu J, Li J, Tran C, Aluri K, Zhang X, Clausen V, Zlatev I, Guan L, Chong S, Charisse K et al. (2019) Oligonucleotide quantification and metabolite profiling by high-resolution and accurate mass spectrometry. *Bioanalysis* **11**:1967–1980.

Nair JK, Attarwala H, Sehgal A, Wang Q, Aluri K, Zhang X, Gao M, Liu J, Indrakanti R, Schofield S et al. (2017) Impact of enhanced metabolic stability on pharmacokinetics and pharmacodynamics of GalNAc-siRNA conjugates. *Nucleic Acids Res* **45**:10969–10977.

Nair JK, Willoughby JL, Chan A, Charisse K, Alam MR, Wang Q, Hoekstra M, Kandasamy P, Kel'in AV, Milstein S et al. (2014) Multivalent N-acetylgalactosamine-conjugated siRNA localizes in hepatocytes and elicits robust RNAi-mediated gene silencing. *J Am Chem Soc* **136**:16958–16961.

Nakanishi K (2016) Anatomy of RISC: how do small RNAs and chaperones activate argonaute proteins? *Wiley Interdiscip Rev RNA* **7**:637–660.

Puy H, Gouya L, and Deybach JC (2010) Porphyrias. *Lancet* **375**:924–937.

Ramsden D, Wu JT, Zerler B, Iqbal S, Jiang J, Clausen V, Aluri K, Gu Y, Dennin S, Kim J et al. (2019) In vitro drug-drug interaction evaluation of GalNAc conjugated siRNAs against CYP450 enzymes and transporters. *Drug Metab Dispos* **47**:1183–1194.

Rocca C, Dennin S, Gu Y, Kim J, Chigas S, Najarian D, Chong S, Gutierrez S, Butler J, Charisse K et al. (2019) Evaluation of electrophoretic mobility shift assay as a method to determine plasma protein binding of siRNA. *Bioanalysis* **11**:1927–1939.

Sardh E, Harper P, Balwani M, Stein P, Rees D, Bissell DM, Desnick R, Parker C, Phillips J, Bonkovsky HL et al. (2019) Phase 1 trial of an RNA interference therapy for acute intermittent porphyria. *N Engl J Med* **380**:549–558.

Setten RL, Rossi JJ, and Han SP (2019) The current state and future directions of RNAi-based therapeutics. *Nat Rev Drug Discov* **18**:421–446.

Wittrup A and Lieberman J (2015) Knocking down disease: a progress report on siRNA therapeutics. *Nat Rev Genet* **16**:543–552.

Address correspondence to: Saeho Chong, Drug Metabolism and Pharmacokinetics, Early Development, Alnylam Pharmaceuticals, 675 W Kendall St., Cambridge, Massachusetts 02142. E-mail: schong@alnylam.com